UVA, no substantial number of apoptotic cells was observed in any of chemicals (Fig. 3A, C, E, G, I, K and M). Necrosis was induced at ~30% with TCSA or bithionol at 10^{-4} M without UVA (Fig. 3B and D), suggesting that they are slightly cytotoxic to keratinocytes at this concentration. Chlorpromazine, diphenylhydramine, 6-methylcoumarin, SPFX, and ENX had no cytotoxic effect on the cells (Fig. 3F, H, J, L and N).

UVA irradiation greatly enhanced the number of early apoptotic cells as compared to non-irradiated cells in TCSA, bithionol and chlorpromazine at 10^{-5} M, and SPFX and ENX at 10^{-4} M (Fig. 3A, C, E, K and M). TCSA, bithionol, and chlorpromazine at 10^{-4} M plus UVA induced necrosis rather than apoptosis (Fig. 3B, D and F), while the quinolone derivatives, SPFX and ENX, minimally induced necrosis even at 10^{-4} M with UVA (Fig. 3L and N). Diphenylhydramine and 6-methylcoumarin at 10^{-4} M had no photoexciting effect on apoptosis or necrosis (Fig. 3G, H, I and J).

3.3. Induction of apoptosis signalings by photosensitizing chemicals and UVA

Caspase activation plays a key role in the process of apoptosis. In particular, caspase-3 is activated during early apoptosis, and its active form is considered to be an excellent marker of cells undergoing apoptosis [18,19]. HaCaT cells were cultured with TCSA, bithionol or chlorpromazine at 10^{-5} M, or SPFX or ENX at 10^{-4} M, with or without UVA exposure. As shown in Fig. 4, without UVA, caspase-3 was not activated in any of the five photosensitizing chemicals. In all chemicals, however, caspase-3 was activated by UVA irradiation at various degrees. Since UVB radiation is well known to activate both the membrane death receptor and the intrinsic or mitochondrial apoptotic signaling pathways in epidermal keratinocytes [20], we compared the apoptotic effect of the chemical/UVA with that of UVB at 60mJ/cm^2. TCSA and chlorpromazine with the help of UVA yielded caspase-3 activation at comparable levels to UVB.

PARP is a substrate for active caspase-3 [19,20]. To further confirm the apoptosis *via* caspase-3, PARP was examined by Western blotting. HaCaT cells were cultured with TCSA, bithionol, or chlorpromazine at 10^{-5} M with or without UVA exposure. As shown in Fig. 5, the treatment of cells with TCSA or chlorpromazine under UVA produced an 85-kDa fragment of cleaved PARP, indicating activation of this molecule.

4. Discussion

In general, photoallergic chemicals have various extents of phototoxic potential, as represented by TCSA [12,13]. On the other hand, there exist some chemicals possessing an exclusively phototoxic moiety, such as psoralen and coal tar [21]. Therefore, photosensitizing chemicals have phototoxic or both phototoxic and photoallergic potentials. Apoptosis is usually considered to be one of the phototoxic outcome [22]. However, given that apoptotic cells bearing certain antigenic chemicals are easily captured and their antigenic determinants are presented by dendritic cells [14,15], apoptosis also seems to be closely related to the immunological response where T cells are primed. Thus, apoptosis induced by photosensitizing agents plus UVA may at least partly reflect photoallergy to a given reagent.

The present study demonstrated that apoptosis of keratinocytes is induced by some of the photosensitizing chemicals that cause photocontact dermatitis and drug photoallergy. Among the chemicals examined here, TCSA has been considered to be one of the strongest photohaptens, as TCSA yields a higher magnitude of murine photocontact dermatitis than bithionol, tribromsalen, musk ambrette, 6-methylcoumarin, benzocaine, hexachlorophene, and sulfanilamide [5]. Accordingly, the ability of TCSA to evoke apoptosis was the highest in our assessment. When determined by the murine contact photosensitivity, chlorpromazine is another drug to possess a strong photosensitizing ability, and bithionol has a moderate potency [5]. We also found that discernible levels of apoptosis were induced by these chemicals. Thus, it is likely that the photoallergic capacity is associated with the apoptosis-inducing ability of photosensitizing chemicals.

We found that caspase-3 activation and PARP expression were induced in HaCaT keratinocytes by treatment with the photosensitizing chemicals plus UVA. In general, apoptosis is induced by a couple of different pathways in which mitochondrial events and Fas/Fas-L stimulation are involved [23]. Although the signaling pathway of apoptosis induced by photosensitizing chemicals remains unfully elucidated, there have been several studies using fluoroquinolones, which are representative chemicals causative for both phototoxic and photoallergic dermatitis [7-10]. Apoptosis by lomefloxacin, a representative fluoroquinolone, is caused by caspase-3 activation and Fas-L induction [24]. In addition, photosensitized lomefloxacin alters mitochondrial membrane [25]. These findings suggest that both pathways involving the Fas/Fas-L and

mitochondrial changes mediate apoptosis by photosensitizing chemicals. Notably, the fluoroquinolones to induce such apoptotic events are highly photoallergic as well [7-10].

Keratinocytes are physiologically exposed to sunlight and capable of responding to UV light to produce cytokines, chemokines, and prostaglandins [26]. Furthermore, the UV effect on keratinocyte apoptosis has been considerably studied [19,20,27]. As demonstrated in this study, TCSA, bithionol, and chlorpromazine, SPFX, and ENX were identified as apoptosis-inducing photosensitizers for keratinocytes. We suggest that this *in vitro* system is one of the useful screening methods to predict both phototoxic and photoallergic potentials of chemicals.

Acknowledgements

This work was supported by a grant from Ministry of Health, Labour and Welfare, Japan (No 040122).

References

[1] Tokura, Y., 2000. Immune responses to photohaptens: implications for the mechanisms of photosensitivity to exogenous agents. J Dermatol Sci. 23, suppl. 6-9.

[2] Harbor, L.C., Harris, H., Baer, R.L., 1966. Photoallergic contact dermatitis due to halogenated salicylanilides and related compounds. Arch Dermatol. 94, 255-262.

[3] Epstein, J.H., Wepper, K.D., Maibach, H.I., 1998. Photocontact dermatitis to halogenated salicylanilides and related compounds; a clinical and histological review of 26 patients. Arch Dermatol. 97, 236-244.

[4] Bosca, F., Miranda, M.A., 1998. Photosensitizing drugs containing the benzophenone chromophore. J Photochem Photobiol B. 43, 1-26.

[5] Miyachi, Y., Takigawa, M., 1983. Mechanisms of contact photosensitivity in mice. III. Predictive testing of chemicals with photoallergic potential in mice. Arch Dermatol. 119, 736-739.

[6] Tokura, Y., Ogai, M., Yagi, H., Takigawa, M., 1994. Afloqualone photosensitivity: immunogenicity of afloqualone-photomodified epidermal cells. Photochem Photobiol. 60, 262-267.

[7] Tokura, Y., 1998. Quinolone photoallergy: photosensitivity dermatitis induced by systemic administration of photohaptenic drugs. J Dermatol Sci. 18, 1-10.

[8] Tokura, Y., Seo, N., Yagi, H., Furukawa, F., Takigawa, M., 1998. Cross-reactivity in murine fluoroquinolone photoallergy: exclusive usage of TCR Vβ13 by immune T cells that recognize fluoroquinolone-photomodified cells. J Immunol. 160, 3719-3728.

[9] Ohshima A, Seo N, Takigawa M, Tokura Y. Formation of antigenic quinolone photoadducts on Langerhans cells initiates photoallergy to systemically administered quinolone in mice. J Invest Dermatol 114: 569-575, 2000.

[10] Tokura Y, Seo N, Fujie M, Takigawa M. Quinolone-photoconjugated MHC class II-bearing peptides with lysine are antigenic for T cells mediating murine quinolone photoallergy. J Invest Dermatol 117, 1206-1211, 2001

[11] Inbaraj, J.J., Kukielczak, B.M., Chignell, C.F., 2005. Phloxine B phototoxicity: a mechanistic study using HaCaT keratinocytees. Photochem Photobiol. 81, 81-88.

[12] Tokura, Y., Takigawa, M., Yamada, M., 1988. Induction of contact photosensitivity to TCSA using photohapten-modified syngeneic spleen cells. Arch Dermatol Res. 280, 207-213.

[13] Tokura, Y., Satoh, T., Yamada, M., Takigawa, M., 1991. In vitro activation of immune lymph node cell proliferaion by photohapten-modified cells in murine contact photosensitivity. Arch Dermatol Res. 283, 203-209.

[14] Scheffer, S.R., Nave, H., Korangy, F., Schlote, K., Pabst, R., Jaffee, E.M., Manns, M.P., Greten, T.F., 2003. Apoptotic, but not necrotic, tumor cell vaccines induce a potent immune response in vivo. Int J Cancer. 103, 205-211.

[15] Edelson R., 2001. Cutaneous T cell lymphoma: the helping hand of dendritic cells, Ann N Y Acad Sci. 941, 1-11.

[16] Boukamp, P., Petrussevska, R.T., Breitkreutz, D., Hornung, J., Markham, A., Fussenig, N.E., 1988. Normal keratinization in a spontaneously immortalized aneuploid human keratinocyte cell line. J Cell Biol. 106, 761-771.

[17] Mancini, M., Nicholson, D.W., Roy, S., Thornberry, N.A., Peterson, E.P., Casciola-Rosen, L.A., Rosen, A., 1998. The caspase-3 precursor has a cytosolic and mitochondrial distribution: implications for apoptotic signaling. J Cell Biol. 140, 1485-1495.

[18] Mancini, M., Nicholson, D.W., Roy, S., Thornberry, N.A., Peterson, E.P.,

Casciola-Rosen, L.A., Rosen, A., 1998. The caspase-3 precursor has a cytosolic and mitochondrial distribution: implications for apoptotic signaling. J Cell Biol. 140, 1485-1495.

[19] Ettore, A., Andreassi, M., Anselmi, C., Neri, P., Andreassi, L., Di Stefano, A., 2003. Involvement of oxidative stress in apoptosis induced by a mixture of isothiazolinones in normal human keratinocytes. J Invest Dermatol. 121, 328-336.

[20] Sitailo, L.A., Tibundan, S.S., Denning, M.F., 2002. Activation of caspase-9 is required for UV-induced apoptosis of human keratinocytes. J Biol Chem. 277, 19346-19352.

[21] Epstein JH. Phototoxicity and photoallergy. Semin Cutan Med Surg 1999 18:274-284.

[22] He, YY., Chignell, CF., Miller, DS., Andley, UP., Roberts, JE., 2004. Phototoxicity in human lens epithelial cells promoted by St. John's Wort. Photochem Photobiol. 80, 583-586.

[23] Kroemer, G., Reed, J.C., 2000. Mitochondrial control of cell death. Nat Med. 6, 513-519.

[24] Marrot, L., Belaidi, J.P., Jones, C., Perez, P., Riou, L., Sarasin, A., Meunier, J.R., 2003. Molecular responses to photogenotoxic stress induced by the antibiotic lomefloxacin in human skin cells: from DNA damage to apoptosis. J Invest Dermatol. 121, 596-606.

[25] Ouedraogo, G., Morliere, P., Santus, R., Miranda, Castell, J.V., 2000. Damage to mitochondria of cultured human skin fibroblasts photosensitized by fluoroquinolones, J Photochem Photobiol B. 58, 20-25.

[26] Takashima, A., Bergstresser, P.R., 1996. Impact of UVB radiation on the epidermal cytokine network. Photochem Photobiol. 63, 397-400.

[27] Assefa, Z., Van, Laethem, A., Garmyn, M., Agostinis, P., 2005. Ultraviolet radiation-induced apoptosis in keratinocytes: on the role of cytosolic factors. Biochim Biophys Acta. 1755, 90-106.

Figure legends

Fig. 1. Fluorescence of TCSA in the membrane and cytoplasm of TCSA-photoconjugated HaCaT cells. HaCaT cells were incubated with TCSA at the indicated concentration or in PBS alone irradiated with UVA at 4 J/cm^2, and observed in a fluorescence microscopy.

Fig. 2. Representative dot-charts of annexin-V/7-AAD bivariate flow cytometry. HaCaT cells were treated with TCSA at the indicated concentration with or without UVA exposure (4 J/cm^2). The lower left quadrant (annexin-/7-AAD -) contains viable cells. The lower right quadrant (annexin+/7-AAD-) represents apoptotic cells. The upper both left and right quadrant (7-AAD+) shows necrotic cells.

Fig. 3. Apoptosis and necrosis in HaCaT cells treated with each chemical plus UVA. HaCaT cells were treated with the indicated chemical and/or UVA. Results were expressed as the mean percentage $\pm$SD of apoptotic and necrotic cells from three independent experiments. *P<0.05, compared with non-irradiated control.

Fig. 4. Activation of caspase-3 in HaCaT cells treated with each chemical plus UVA. Data represent the percentage (mean$\pm$SD, n=3) of active caspase-3-positive cells induced by TCSA, bithionol or chlorpromazine at 10^{-5} M, or SPFX or ENX at 10^{-4} M with or without UVA (4 J/cm^2). *P<0.05, **P<0.01, compared with non-irradiated control cells. As a positive control, HaCaT cells were irradiated with UVB (60 mJ/cm^2) (n=3, mean$\pm$SD).

Fig. 5. Expression of PARP in HaCaT cells treated with each chemical plus UVA. HaCaT cells were treated with TCSA, bithionol, or chlorpromazine at 10^{-5} M with or without UVA at 4 J/cm^2. As positive and negative control, UVB (60 mJ/cm2) irradiated or non-treated HaCaT cells were used. Cell lysates were collected 12 hr after irradiation.

Table 1

Chemical materials used in this study

Chemicals	Source	Structure	Usage
3, 3', 4' 5-tetrachlorosalicylanilide (TCSA)	Eastman Kodak, Rochester, N.Y.	Cl2C6H2(OH)CONHC6H3Cl2	Anti-microbial agent
Bithionol	Sigma-Aldrich, Milano, Italy	C12H6Cl4O2S	Anti-microbial agent
6-methlcoumarin	Wako Chemical Co., Tokyo, Japan	CH3C6H3OCOCH:CH	Perfume
Diphenhydramine	Sigma-Aldrich, Milano, Italy	C17H21NO·HCl	Anti-histamic drug
Chlorpromazine	Sigma-Aldrich, Milano, Italy	C17H21NO·HCl	Major tranquilizer
Spafloxacin (SPFX)	Dainippon Sumitomo Pharma Co., Osaka, Japan	C19H22F2N4O3	Anti-microbacterial quinolone
Enoxacin (ENX)	Dainippon Sumitomo Pharma Co., Osaka, Japan	C15H17FN4O3·1 1/2H2O	Anti-microbacterial quinolone

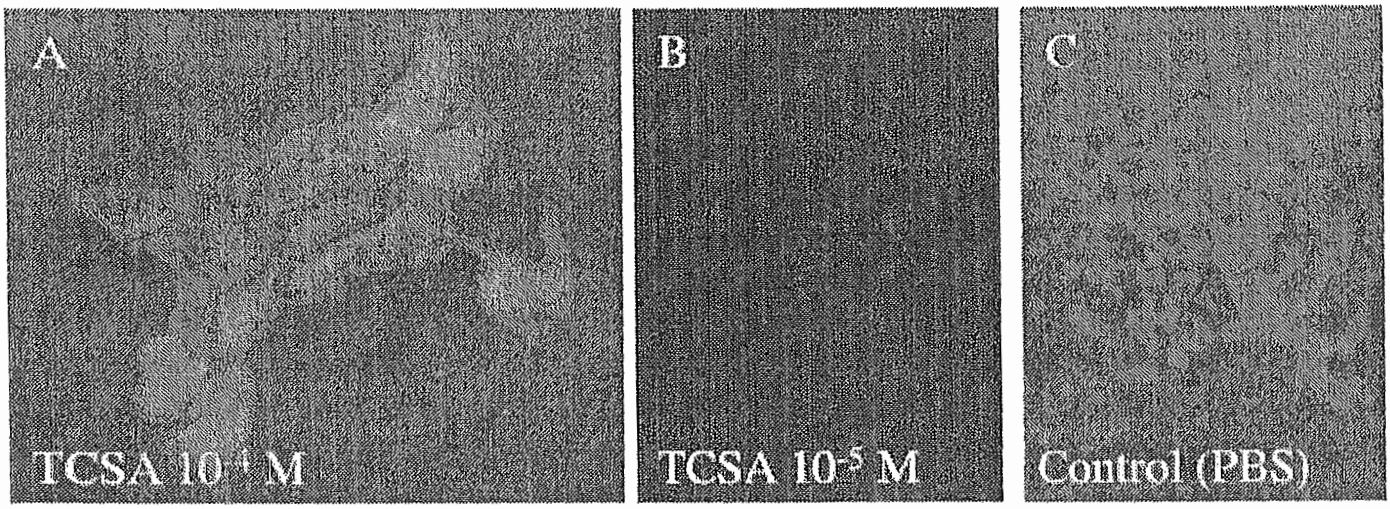

Fig. 1

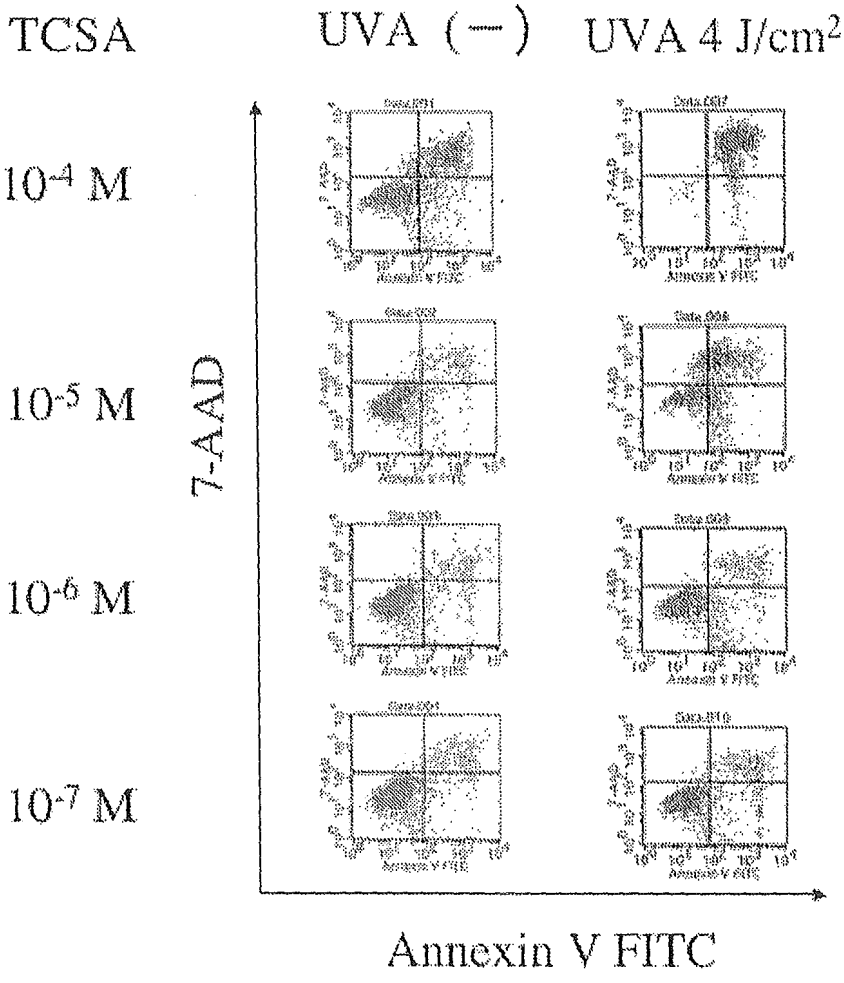

Fig. 2

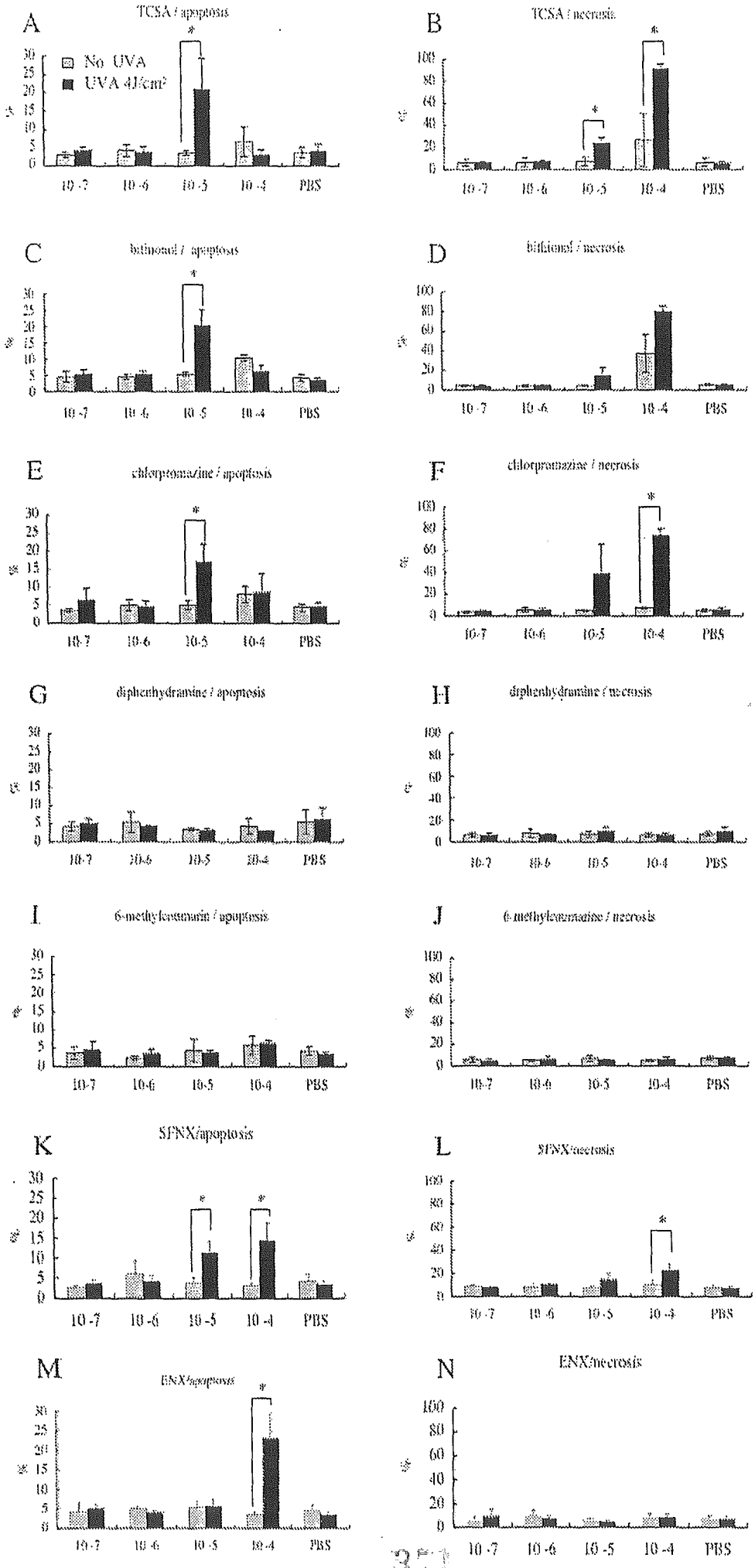
A
TCSA / apoptosis
No UVA
UVA 4J/cm²
B
TCSA / necrosis
C
bithionol / apoptosis
D
bithionol / necrosis
E
chlorpromazine / apoptosis
F
chlorpromazine / necrosis
G
diphenhydramine / apoptosis
H
diphenhydramine / necrosis
I
6-methylcoumarin / apoptosis
J
6-methylcoumarin / necrosis
K
SFNX/apoptosis
L
SFNX/necrosis
M
ENX/apoptosis
N
ENX/necrosis
10-7
10-6
10-5
10-4
PBS

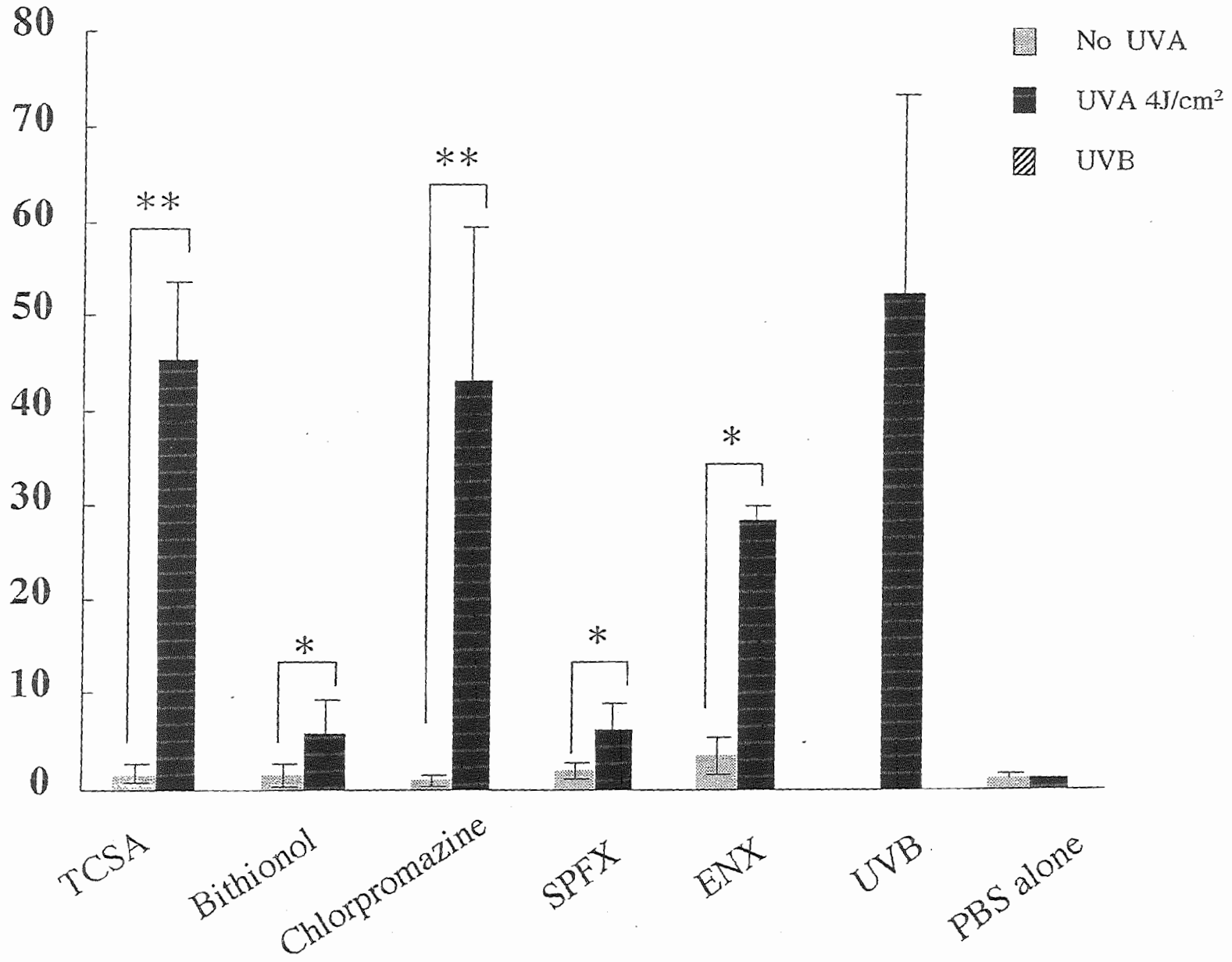
80
70
60
50
40
30
20
10
0
No UVA
UVA 4J/cm²
UVB
**
**
*
*
*
TCSA
Bithionol
Chlorpromazine
SPFX
ENX
UVB
PBS alone

Fig. 4

PARP
116 kDa
85 kDa
UVB
Chlorpromazine+UVA
Chlorpromazine
Bithionol+UVA
Bithionol
TCSA+UVA
TCSA
Control
M

Fig. 5

SETAC PRESS

Environmental Toxicology and Chemistry, Vol. 24, No. 8, pp. 1984–1993, 2005

Printed in the USA
0730-7268/05 $12.00 + .00

PRESENCE AND ESTROGENICITY OF ANTHRACENE DERIVATIVES IN COASTAL JAPANESE WATERS

RYO KURIHARA,† FUJIO SHIRAISHI,‡ NORIHO TANAKA,§ and SHINYA HASHIMOTO*†
†Laboratory of Ecological Chemistry, Institute for Environmental Sciences, University of Shizuoka, Shizuoka 422-8526, Japan
‡National Institute for Environmental Studies, Ibaraki 305-8506, Japan
§Hadano Research Institute, Food and Drug Safety Center, Kanagawa 257-8523, Japan

(*Received* 22 *June* 2004; *Accepted* 28 *January* 2005)

Abstract—An analytical method was developed to measure levels of anthracene (ANT) and its derivative compounds 9,10-anthraquinone (ATQ) and eight hydroxy-anthraquinones (hATQs) in seawater from Tokyo Bay and Suruga Bay, Japan. The hATQs produced through photochemical reaction of ANT are known to be toxic. Seawater samples contained ANT at levels ranging from <0.2 to 4.7 ng/L, ATQ from 3.9 to 200 ng/L, 1-hydroxyanthraquinone (1-hATQ) from <0.9 to 5.3 ng/L, and 2-hATQ from 1.6 to 5.5 ng/L. The yeast two-hybrid system was also used to evaluate the estrogenic activity of these compounds. Estrogen agonist and antagonist tests with or without rat liver S9 were carried out. Some compounds showed estrogenic activity: The strongest (2-hydroxyanthraquinone) was of similar potency to *p*-nonylphenol. Concentrations of some estrogenic derivatives in the samples were higher than those of the parent ANT. Polycyclic aromatic hydrocarbons (PAHs) such as ANT appear able to be transformed into toxic compounds in the environment when they are irradiated by sunlight, so it is important to monitor not only PAHs but also hydroxyl-PAH-quinones in the environment.

Keywords—Anthracene derivatives Hydroxy-anthraquinones Photochemical reaction Marine environment Estrogenicity

INTRODUCTION

Petroleum is the world's most important energy source. One of the drawbacks of oil spills is marine pollution, a serious environmental problem. If these spills remain in the environment, marine organisms are exposed to the chemical compounds in them, with disastrous effects, particularly after tanker accidents [1,2]. Polycyclic aromatic hydrocarbons (PAHs) are environmental contaminants that are present in petroleum and form as by-products of the incomplete combustion of organic compounds. Polycyclic aromatic hydrocarbons can be detected in the atmosphere [3], marine core sediments [4], and living organisms [5] and have spread all over the world. Many reports have been made of intact PAHs in the environment [3–5]. Exposure to light results in photochemical reactions that enhance the toxicity of PAHs [6–9], and they can form photochemical reaction products, such as hydroxyl-PAH-quinones, that have greater toxicity than the parent compounds. For these reasons, it is important to study the environmental existence and toxicity of PAHs and their derivatives.

The present study focused on the PAH anthracene (ANT), some of whose photochemical reaction products have greater toxicity to higher plants than ANT itself [8]. These photochemical reaction products include 9,10-anthraquinone (ATQ), hydroxy-anthraquinones (hATQs), and lower-molecular-weight compounds [10]. The reaction pathways of these compounds have been proposed in previous literature [10]. When ANT is irradiated with simulated solar radiation (SSR), it is converted mainly to ATQ via an intermediate. The intermediate has been proposed to be the 9,10-endoperoxide of ANT [10]. The ATQ is then hydroxylated to hATQs, such as 1-hATQ or 2-hATQ. Derivatives of ATQ are important materials in industrial [11] and medical [12] applications, and their toxicities have been reported in a previous study [13].

To the best of our knowledge, little information exists on the photochemical reaction products of ANT in the environment. The amounts of ANT and ATQ in coastal marine sediments from sites in the northeastern United States have been reported [14], although the environmental existence of 1-hATQ [15] and 2-hATQ [16] has been reported only by preliminary analysis.

Many natural and synthetic compounds, such as 17β-estradiol, estrone, 17-ethinylestradiol, diethylstilbestrol, *p*-nonylphenol, and bisphenol A, are known to have estrogenic activity [17]. Recently, some hydroxylated environmental pollutants have been found to be estrogenic, for example, hydroxylated benzophenones [18], polychlorinated biphenyls [19], and PAHs [20]. The photochemical reaction products of ANT have variable toxicity and carcinogenicity to organisms such as higher plants and August Copenhagen Irish rats [8,13]. Photosensitization and photomodification of PAHs are mechanisms related to the enhancement of toxicity, and it is therefore important to evaluate the estrogenic activity of both the primary compounds and their photochemical reaction products. Although some hydroxyl-PAHs have been reported to interact with estrogen receptors and show weak estrogenic activity [20], the estrogenicity of such ANT derivatives has never been fully investigated.

Receptor-binding assays, a Michigan Cancer Foundation-7 (MCF-7) cell proliferation assay (estrogen screen, E-screen), and reporter gene assays in animal cell lines have recently been developed as in vitro screening techniques to evaluate estrogenic activity [21]. The yeast two-hybrid system is a popular method. A recently developed yeast two-hybrid assay has

* To whom correspondence may be addressed (hashimos@u-shizuoka-ken.ac.jp).

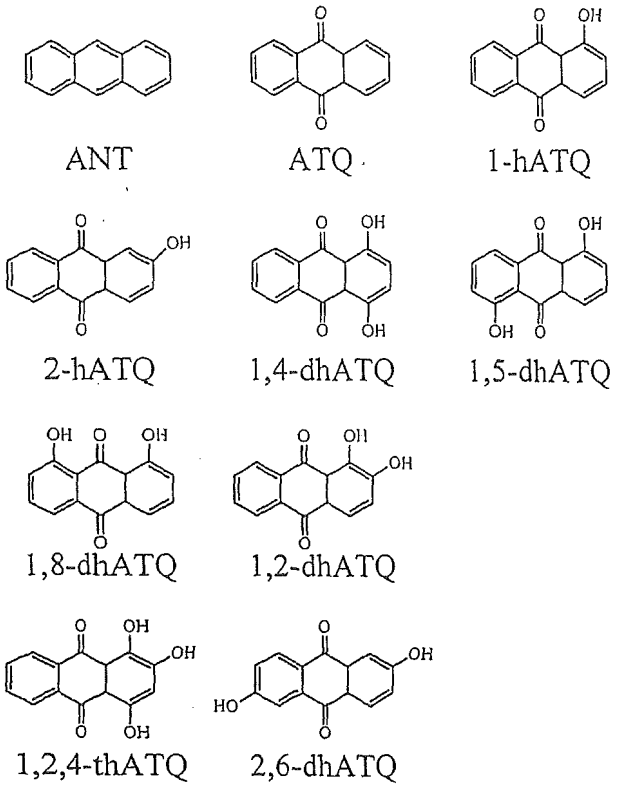

Fig. 1. Structures of anthracene (ANT) and nine of its derivatives used: ATQ = 9,10-anthraquinone; 1-hATQ = 1-hydroxyanthraquinone; 2-hATQ = 2-hydroxyanthraquinone; 1,4-dhATQ = quinizarin; 1,5-dhATQ = anthrarufin; 1,8-dhATQ = danthron; 1,2-dhATQ = alizarin; 1,2,4-thATQ = purpurin; 2,6-dhATQ = anthraflavic acid.

attracted attention because it allows detection of the presence of endocrine disruptors in a relatively short period of time [17]. Subsequently, a modified method has been developed as a more rapid and simpler detection system [22].

Our primary objective was to develop a method of determining the concentrations of ANT and its photochemical reaction products, including hATQs, in seawater and to use it to test seawater samples off the coast of Japan. Our secondary objective was to evaluate the estrogenic activity of the photochemical reaction products of ANT and their contribution to environmental estrogenic contamination.

MATERIALS AND METHODS

Chemicals

The structures and abbreviations of our target compounds are shown in Figure 1. Anthracene (99% pure), ATQ (97% pure), quinizarin (1,4-dihydroxyATQ; 96% pure), anthrarufin (1,5-dhATQ; 85% pure), danthron (1,8-dhATQ; 96% pure), alizarin (1,2-dhATQ; 97% pure), purpurin (1,2,4-trihATQ; 90% pure), and anthraflavic acid (2,6-dhATQ; 90% pure) were purchased from Sigma-Aldrich (Tokyo, Japan). The 1-hATQ (>95% pure) and 2-hATQ (90% pure) were purchased from Tokyo Kasei Kogyo (Tokyo, Japan). These reagents were used without further purification. Pesticide residue grade solvents and chemicals were obtained from Wako Chemical (Tokyo, Japan).

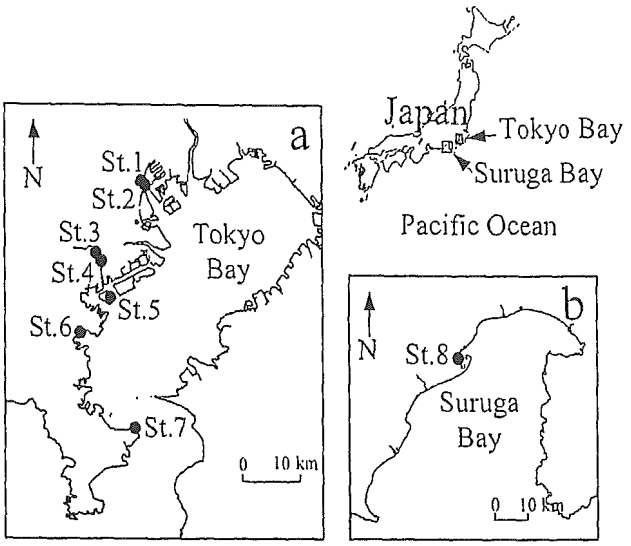

Fig. 2. Sampling locations: (a) Tokyo Bay and (b) Suruga Bay, Japan. Seawater was collected at stations 1 to 8.

Study sites and water collection

Tokyo Bay, with a surrounding population of nearly 26 million, is one of the most polluted areas in the world and has been the subject of many studies of environmental contaminants. For example, studies of fluorescent whitening agents [23] and haloacetic acid [24] have been reported in the past decade. Additionally, histological abnormalities in the gonads of konoshiro gizzard shad (*Konosirus punctatus*) [25] and flounder (*Pleuronectes yokohamae*) [26] were found in samples from inner areas of Tokyo Bay. For our current study, surface seawater samples from Tokyo Bay and Suruga Bay were collected in a stainless-steel bucket. The sampling sites are shown in Figure 2, and their latitude, longitude, collection date, depth, water temperature, and pH are shown in Table 1. Precleaned brown glass bottles (5,000 ml) were rinsed with seawater three times, then filled with sample water and capped.

Table 1. Sampling locations and characteristics of seawater samples (Japan)

Sampling station	Location	Collection date	Depth (m)	WT[a] (°C)	pH
1	35°37.894′N, 139°45.044′E	July 16, 2003	5.0	24.2	6.8
2	35°37.690′N, 139°45.445′E	July 16, 2003	2.1	23.2	7.0
3	35°31.008′N, 139°40.766′E	July 16, 2003	2.9	22.8	7.0
4	35°30.678′N, 139°41.031′E	July 16, 2003	2.7	23.0	6.9
5	35°27.362′N, 139°41.450′E	July 16, 2003	4.1	25.6	8.2
6	35°24.133′N, 139°38.282′E	July 16, 2003	3.5	24.8	8.3
7	35°15.309′N, 139°44.678′E	July 16, 2003	1.3	22.1	8.3
8	35°00.311′N, 138°30.034′E	June 27, 2003	12.2	24.2	8.1

[a] Water temperature.

Samples were brought to the laboratory within 1 d and stored at 4°C.

Chemical analysis procedure

Chemical analysis was performed with a gas chromatograph (GC; HP 5890 series II, Agilent Technologies, Wilmington, DE, USA) mass spectrometer (MS; HP5971 MSD) using selected ion monitoring. Standard and sample extract solutions were analyzed by injecting 1 μl of solution using a 7673-series autoinjector (Agilent Technologies). Separation was done in a 30-m DB-5MS capillary column (0.25-mm i.d., 0.25-μm film, J&W Scientific, Folsom, CA, USA). The GC oven temperature was programmed with a starting temperature of 90°C for 2 min, followed by a 10°C/min temperature increase to a final temperature of 290°C, which was held for 5 min. Identification was made by retention times and ion ratios. The hATQs were detected after trimethylsilylation with *N,O*-bis(trimethylsilyl)trifluoroacetamide with 10% trimethylchlorosilane ([BSTFA] + 10% TMCS, Pierce, Rockford, IL, USA). Standardization was done with anthracene-d_{10} for all the compounds. Silylation reaction time was optimized and found to be 60 min.

The rates of recovery of the target compounds were also optimized. Each test compound was dissolved in acetonitrile to 5 mg/L, and 100 μl of this solution were added to 500 ml of seawater from Suruga Bay (station 8) to give a final concentration of 1 μg/L of each test compound. The 500 ml of spiked seawater were filtered through a glass microfiber filter GF/C 47 mm (Whatman International, Maidstone, UK) and extracted by a 47-mm solid-phase Empore disk (3M, St. Paul, MN, USA), either after acidification with 1 ml concentrated HCl to about pH 2 or with no acidification. Two solid-phase disks, octadecyl silica (C_{18}) [27] and polystyrene–divinylbenzene copolymer (SDB-XC) [28], were used for the extraction. The solid-phase disks were cleaned with 5 ml dichloromethane, 5 ml methanol, and Milli-Q® water (Millipore, Bedford, MA, USA). After the seawater had been extracted by the solid phase, the target compounds were eluted with 5 ml acetone and 15 ml dichloromethane. The extract was filtered and dehydrated by passage through a column of anhydrous sodium sulfate. The organic solution was concentrated in a rotary evaporator, and the solvent was changed to acetonitrile under a nitrogen stream at less than 28°C. After derivatization of the sample with BSTFA (50 μl), the concentrations of ANT and its derivatives were measured by means of GC-MS. The extraction procedure was done in triplicate.

Application of the procedure for measurement of ANT and its derivatives in seawater

We used 1,000 ml of seawater to detect ANT and its derivatives. Ultimately, the organic layer was concentrated to 200 μl. In the case of the sample extraction by means of the C_{18} disk, half of each sample was used for the analysis of ANT and ATQ. The BSTFA was not added to these samples because BSTFA increased the background level of the chromatogram. The rest of the concentrated organic layer was used for the analysis of 1-hATQ, 1,5-dhATQ, and 1,8-dhATQs after derivatization with BSTFA (50 μl). Similarly, the samples extracted by SDB-XC were used for analysis of 2-hATQ, 1,4-dhATQ, 1,2-dhATQ, 1,2,4-thATQ, and 2,6-dhATQs. Each sample was measured in duplicate or triplicate.

Stability of ANT and its derivatives in seawater

The stability of ANT and its derivatives stored in seawater was examined by modifying the methods that are used for the study of estradiol and ethinylestradiol degradation [29]. Briefly, the ANT and its derivatives (each concentration: 1 μg/L) were incubated in the dark at 20.0 ± 0.15°C in precleaned glass bottles with seawater collected at station 8, and the concentrations of these compounds were measured in a 1,000-ml sample 0, 2, 4, 8, and 24 d after incubation began.

Estrogenicity assay

We used a rapid and simple operational estrogenicity assay system with the yeast two-hybrid system, based on the ligand-dependent interaction of two proteins (a hormone receptor and a coactivator), and detected hormonal activity on the basis of β-galactosidase activity [22,30,31]. Recombinant yeast with the estrogen receptor ERα and coactivator TIF2 was provided, and a method of screening for chemicals with hormonal activity was developed using the yeast Y190 (selected by growth on medium lacking tryptophan and leucine) in which two expression plasmids, the pGBT9-estrogen receptor ligand-binding domain (pGBT9-ER LBD) and pGAAD424-TIF2, were introduced [32]. Subsequently, we developed a modified procedure to simplify this method and improve its sensitivity by adapting the 96-well plate-culture method and the chemiluminescent reporter-gene assay method [22]. An Aurora GAL-XE kit containing chemiluminescent substrate, reaction buffer, and accelerator was purchased from ICN Pharmaceuticals (Costa Mesa, CA, USA). Zymolyase 20T was purchased from Seikagaku (Tokyo, Japan). Rat liver S9 was purchased from Kikkoman (Tokyo, Japan).

The estrogen agonist activities of ANT, ATQ, and the eight hATQ compounds in Figure 1 were examined. In addition, the activities of other low-molecular-weight photochemical reaction products of ANT, such as 2,5-dihydroxybenzoic acid, 2-hydroxy-1,4-naphthoquinone, and salicylaldehyde, were assessed [10]. Anthrarobin, 2-hydroxydibenzofuran, 2-hydroxyfluorene, 2-hydroxy-9-fluorenone, and 9-phenanthrol were also assessed to compare the estrogenic activities of target compounds with those of other hydroxyl-PAHs; 2-hydroxydibenzofuran, 2-hydroxyfluorene, and 2-hydroxy-9-fluorenone have been reported to have estrogenic activity [20]. Differences in the intensity of the chemiluminescent signal between samples (four or more times) and a blank control were tested by means of one-way analysis of variance (ANOVA). The chemiluminescent signals were significantly higher in the samples (four or more times) than that of the blank control ($p < 0.002$, ANOVA). Therefore, we defined a positive agonist as occurring when the target chemical increased the chemiluminescent signal to four or more times that with a blank control.

To evaluate the estrogenic activity of the metabolites of test chemicals, we also carried out an estrogenicity assay with S9 metabolic activation using rat liver S9. To analyze the estrogenic activity of the metabolic compounds, we also performed the +S9 test based on rat liver S9. The result of our bioassay of the S9 fraction indicated the estrogenic activity of the metabolic compounds.

Antagonistic assay

We used an antagonist assay system for estrogen receptors that employ a yeast two-hybrid system in which a yeast toxicity test (Ytox test) is incorporated. The principle of the yeast antagonist test for estrogen receptor is measurement of the inhibition of expression of β-galactosidase by competitive estrogen receptor–binding reaction between the test chemical substance and 17β-estradiol added to the medium at 300 pM

Table 2. Ions used for identification and quantification and retention times (RTs) for anthracene (ANT) and its derivatives in seawater

Analyte	Molecular ion/ characteristic fragment ion (*m/z*)[a]	Qualifier ion (*m/z*)	RT (min)
Anthracene	178.1	152.1	13.77
Anthraquinone (ATQ)	208.2	152.1/180.1	15.71
1-Hydroxyanthraquinone (1-hATQ)	281.2	282.2	18.40
2-Hydroxyanthraquinone (2-hATQ)	281.3	282.2/296.3	19.25
Quinizarin (1,4-dhATQ)	354.2	369.2	20.17
Anthrarufin (1,5-dhATQ)	354.2	369.2	20.52
Danthron (1,8-dhATQ)	369.2	370.3	20.67
Alizarin (1,2-dhATQ)	369.2	370.3	20.93
Purpurin (1,2,4-thATQ)	442.3	443.3/457.3	21.81
Anthraflavic acid (2,6-dhATQ)	369.2	384.3	22.20

[a] The *m/z* values correspond to the trimethylsilyl derivatization of the compounds if free hydroxy groups are present.

as a ligand for the receptor [31]. The yeast toxicity test, which measures the residual activity of β-galactosidase using a test chemical alone, is designed to indicate the toxicity of a test chemical to yeast. Thus, general toxicity and estrogen receptor antagonist activity can be distinguished by comparing the two results. The yeast used in the toxicity test has the activity of producing β-galactosidase without estrogen. Where a test chemical is not toxic to yeast, the β-galactosidase activity increases even in the absence of estrogen. Where a test chemical is toxic to yeast, the expression of β-galactosidase decreases. Therefore, a decrease in the expression of β-galactosidase in the Ytox test means that the test chemical was toxic to yeast. We defined the test chemical as an estrogen antagonist when the median effective concentration (EC50) value was less than 25% of the median inhibitory concentration (IC50) value in the Ytox test. We used the estrogen receptor yeast antagonist test to examine the estrogen receptor antagonist activities of ANT and its derivatives. A positive antagonist was defined as a chemical that decreased the chemiluminescent signal to 60% or less of that value for a blank control.

Vibrio *assay*

The toxicity test based on the response of *Vibrio fischeri* (the VF test) measures the inhibition of bacterial luminescence by test substances. We also performed the VF test to detect acute toxicity of the test chemicals. This test was performed as described previously [33].

Briefly, the *V. fischeri* cultures were seeded into a 96-well culture plate with T medium prepared with peptone, glycerol, NaCl, $MgSO_4$, KCl, and K_2HPO_4. Assays were established in triplicate with the test chemicals and blank (T medium containing 4% dimethyl sulfoxide). The intensity of chemiluminescence was measured with an AB2100 Luminescencer (ATTO, Tokyo, Japan). Chemicals were defined as nonactive if the luminescent signal remained between 90 and 100% of the level measured for the control. Differences in the intensity of the chemiluminescent signal between the samples (80–89%) and the blank control were tested by means of ANOVA. The chemiluminescent signals were lower in the samples (80–89%) than in the blank control ($p < 0.05$, ANOVA). Therefore, weak was defined as a statistically significant effect at a concentration of 10μM.

Data analysis

We applied a sigmoidal dose–response regression model to calculate EC50 using the GraphPad Prism 4® software (Ver 4.02; GraphPad Software, San Diego, CA, USA). The EC50 is the concentration at which the chemiluminescent signal of 17β-estradiol was inhibited by 50%. The 10× is the concentration at which the ratio of the chemiluminescent signal of the sample to that of a blank control equals 10. The IC50 values (the concentration at which the chemiluminescent signal was inhibited by 50%) were calculated for those chemicals that inhibited the luminescent signal to a value equal to 0 to 79% of the control value. Statistical analysis of the chemiluminescence results was tested by means of ANOVA. We used Bonferroni posttest to identify the concentrations that are significantly different from the control.

RESULTS

Chemical analysis of ANT and its derivatives

The ions we monitored and their retention times (RTs) are shown in Table 2. The recovery rates of each compound, together with the solid-phase disk used and the detection limit, are presented in Table 3. The recovery rates of some compounds were increased by acidification. For example, the recovery rates without acidification of seawater were 77.5% (1-hATQ), 50.9% (2-hATQ), 21.2% (1,4-dhATQ), 32.9% (1,5-dhATQ), 51.0% (1,8-dhATQ), 18.2% (1,2-dhATQ), 0.0% (1,2,4-thATQ), and 8.2% (2,6-dhATQ). Recovery rates with acidification from test samples from station 8 at Suruga Bay are shown in Table 3. Thus, acidification of seawater increased the recovery rate of hATQs.

The analytical procedure used to detect each compound is summarized in Figure 3. Target compounds were extracted from seawater by using two different solid-phase disks. The results indicated that extraction with both C_{18} and SDB-XC was needed for the measurement of these compounds in seawater. Therefore, we developed an analytical procedure that involved both the acidification of seawater before solid-phase extraction and the use of both C_{18} and SDB-XC disks. The recovery rates of some compounds varied with the disk used. For instance, when 1,8-dhATQ was extracted by SDB-XC, the recovery rate was 38.1% (100% with C_{18}; Table 3). On the other hand, when 1,2-dhATQ and 1,2,4-thATQ were extracted

Table 3. Mean recovery values and detection limits (DLs) of anthracene (ANT) and its derivatives from samples taken from station 8 in Suruga Bay (Japan)[a]

Compound[b]	Solid phase	Recovery rate[c] (%; n = 3)	DL (ng/L)[d]
ANT	C_{18}[e]	78.2 (±0.6)	0.2
ATQ	C_{18}	109 (±7.3)	2.9
1-hATQ	C_{18}	111 (±3.6)	0.9
2-hATQ	SDB-XC[f]	108 (±7.6)	1.2
1,4-dhATQ	SDB-XC	86.3 (±12.2)	0.4
1,5-dhATQ	C_{18}	101 (±0.8)	0.5
1,8-dhATQ	C_{18}	100 (±2.1)	0.8
1,2-dhATQ	SDB-XC	90.2 (±16.0)	1.8
1,2,4-thATQ	SDB-XC	149 (±27.3)	4.8
2,6-dhATQ	SDB-XC	137 (±17.1)	0.4

[a] After acidification with 1 ml concentrated HCl to about pH 2.
[b] ANT = anthracene; ATQ = anthraquinone; 1-hATQ = 1-hydroxyanthraquinone; 2-hATQ = 2-hydroxyanthraquinone; 1,4-dhATQ = quinizarin; 1,5-dhATQ = anthrarufin; 1,8-dhATQ = danthron; 1,2-dhATQ = alizarin; 1,2,4-thATQ = purpurin; 2,6-dhATQ = anthraflavic acid.
[c] Determined from spiked seawater (1 μg/L) using an Empore disk, followed by derivatization with *N,O*– bis(trimethylsilyl)trifluoroacetamide (BSTFA) and gas chromatographic/mass spectrometric analysis.
[d] Signal-to-noise ratio of 3 : 1 was define as being the detection limit.
[e] C_{18} = octadecyl silica.
[f] SDB-XC = polystyrene–divinylbenzene copolymer.

by C_{18}, the recovery rates were 34.5% (90.2% with SDB-XC; Table 3) and 5.9% (149% with SDB-XC; Table 3), respectively.

We used a 1,000-ml sample of Milli-Q water (n = 3) as a blank. No target compound peaks were observed in the chromatogram of this blank, confirming that no contamination occurred during the extraction procedure.

Concentration of ANT and its derivatives in seawater

Table 4 shows the concentrations of ANT, ATQ, and the eight hATQs in seawater from Tokyo Bay and Suruga Bay. Anthracene, ATQ, and four hATQs were detected in the seawater. These compounds were present at concentrations in the order of nanograms per liter in the sampled areas. The ATQ was detected at high concentrations at stations 3 and 4, where low conductivity was measured (station 3: 5.8 ms/cm, station 4: 9.8 ms/cm). Concentrations of ATQ, 2-hATQ, and 2,6-dhATQ were higher than those of the parent compound ANT, except at stations 2 and 4. The relative molar amount of ATQ ranged from 5.6 to 120 times higher, 2-hATQ from 0.74 to 5.4

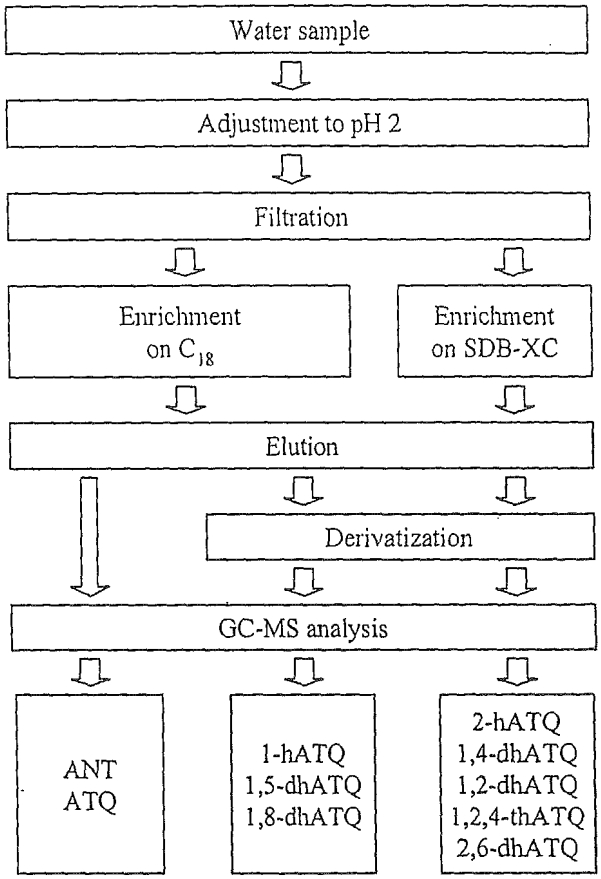

Fig. 3. Analytical procedure used to determine concentrations of anthracene (ANT) and its derivatives in seawater. C_{18} = octadecyl silica; SDC-XC = polystyrene–divinylbenzene copolymer; GC-MS = gas chromatography/mass spectrometry; ANT = anthracene; ATQ = 9,10-anthraquinone; 1-hATQ = 1-hydroxyanthraquinone; 2-hATQ = 2-hydroxyanthraquinone; 1,4-dhATQ = quinizarin; 1,5-dhATQ = anthrarufin; 1,8-dhATQ = danthron; 1,2-dhATQ = alizarin; 1,2,4-thATQ = purpurin; 2,6-dhATQ = anthraflavic acid.

Table 4. Concentration of anthracene (ANT) and its derivatives in seawater from Tokyo Bay and Suruga Bay (Japan) (ng/L)[a]

Compound analyzed[b]	Sampling location (station)[c] 1	2	3	4	5	6	7	8
ANT	2.2	4.7	1.4	1.7	0.4	0.4	BD[d]	0.4
ATQ	42	31	190	200	9.0	6.7	3.9	22
1-hATQ	1.9	BD	5.3	4.4	BD	BD	BD	BD
2-hATQ	3.6	4.4	4.4	5.5	2.7	2.6	1.7	1.6
1,4-dhATQ	BD	BD	BD	BD	BD	BD	BD	BD
1,5-dhATQ	BD	BD	BD	BD	BD	BD	BD	BD
1,8-dhATQ	BD	BD	0.9	BD	BD	BD	16	7.1
1,2-dhATQ	BD	BD	BD	BD	BD	BD	BD	BD
1,2,4-thATQ	BD	BD	BD	BD	BD	BD	BD	BD
2,6-dhATQ	3.4	7.0	2.0	1.7	1.1	1.4	0.6	1.4

[a] Values were averages of concentration found in double or triplicate analysis.
[b] ATQ = anthraquinone; 1-hATQ = 1-hydroxyanthraquinone; 2-hATQ = 2-hydroxyanthraquinone; 1,4-dhATQ = quinizarin; 1,5-dhATQ = anthrarufin; 1,8-dhATQ = danthron; 1,2-dhATQ = alizarin; 1,2,4-thATQ = purpurin; 2,6-dhATQ = anthraflavic acid.
[c] See Figure 2 for details.
[d] BD = below the limit of detection.

Table 5. Degradation rates for 1-μg/L target compounds in seawater from a sample at station 8 at 20°C

Compound[a]	Half-life (d)[b]	Adjusted r^2
ANT	8.9	0.953
ATQ	240	0.851
1-hATQ	5.0	0.961
2-hATQ	5.1	0.925
1,4-dhATQ	2.5	0.979
1,5-dhATQ	20	0.972
1,8-dhATQ	3.1	0.965
1,2-dhATQ	4.7	0.909
1,2,4-thATQ	0.3	0.894
2,6-dhATQ	3.9	0.915

[a] ANT = anthracene; ATQ = anthraquinone; 1-hATQ = 1-hydroxyanthraquinone; 2-hATQ = 2-hydroxyanthraquinone; 1,4-dhATQ = quinizarin; 1,5-dhATQ = anthrarufin; 1,8-dhATQ = danthron; 1,2-dhATQ = alizarin; 1,2,4-thATQ = purpurin; 2,6-dhATQ = anthraflavic acid.

[b] Calculated for target compounds as a simple first-order model.

times higher, and 2,6-dhATQ from 0.74 to 2.6 times higher than ANT values observed at stations 1 to 8.

Stability of ANT and its derivatives in seawater

The stability of ANT and its derivatives were analyzed in seawater collected at station 8. Table 5 shows the half-lives of ANT and its derivatives in seawater. The results indicated that ATQ was the most stable compound in the seawater. Concentrations of eight of the compounds (excluding ATQ and 1,5-dhATQ) decreased to less than 20% of their initial values after 24 d. Concentrations of ANT, 2-hATQ, and 2,6-dhATQ decreased only slightly during the first 8 d, then decreased rapidly. The slight decrease during the first 8 d may reflect the length of time taken for the microbial system to adapt sufficiently to be able to efficiently decompose these compounds. Similar results were obtained in a decomposition experiment that studied anthracene in soil [34].

Estrogen agonist activities of ANT and its derivatives

Figure 4a and b and Table 6 show the estrogen agonist activities of ANT and its photochemical reaction products. The 10× is the concentration at which the ratio of the chemiluminescent signal of the sample to that of a blank control was 10. The positive controls were 17β-estradiol for the −S9 test and *trans*-stilbene for the +S9 test. No activity of *trans*-stilbene occurs in this assay without S9 metabolic activation [17]. Of the ANT derivatives, 2-hATQ and 1,2-dhATQ showed estrogen agonist activity, with 2-hATQ having the strongest activity. We detected 2-hATQ at the test areas (Table 4). The estrogenic activity of 2-hATQ was similar to that of *p*-nonylphenol (10× = 1.2 ×10^5 ng/L) [22], a well-known environmental estrogen. The environmental concentrations of 2-hATQ were lower than that of *p*-nonylphenol (e.g., in Tamagawa River water entering Tokyo Bay, 50–170 ng/L [35]). However, PAHs and their derivatives become significant toxic chemicals that are already present as contaminants in petroleum and that form as by-product of the incomplete combus-

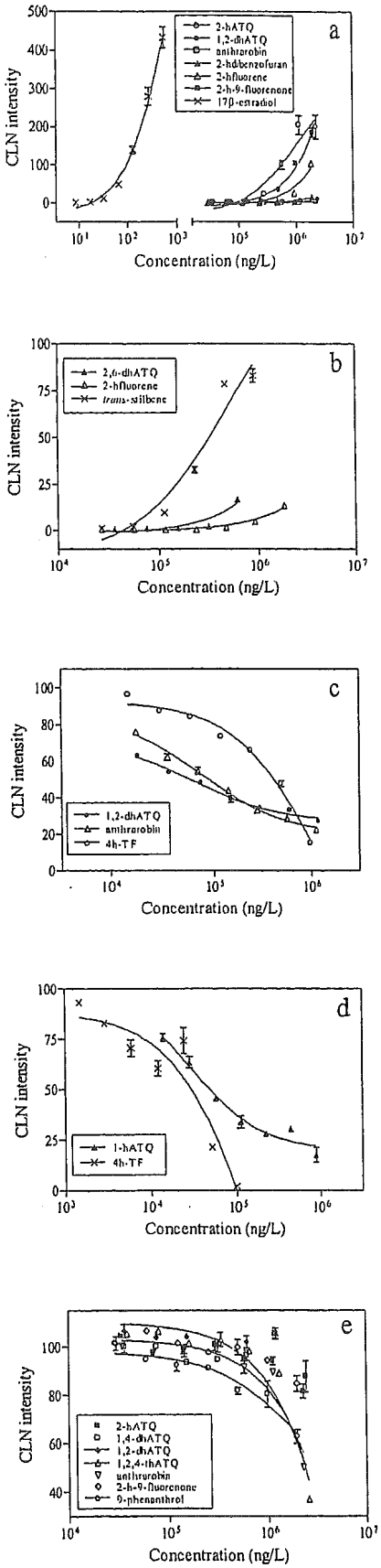

Fig. 4. Dose–response curves of our target compounds and positive controls. (a) Estrogen agonist −S9 test. (b) Estrogen agonist +S9 test. (c) Estrogen antagonist −S9 test. (d) Estrogen antagonist +S9 test. (e) *Vibrio fischeri* (VF) test. CLN intensity = chemiluminescence intensity, defined as the ratio of the CLN value for a sample to the CLN value of the control. The CLN value of the control equals 1.0 in Figures 4a and b and 100 in Figures c to e. 2-hATQ = 2-hydroxyanthraquinone; 1,2-dhATQ = alizarin; 2,6-dhATQ = anthraflavic acid; 1-hATQ = 1-hydroxyanthraquinone; 1, 4-dhATQ = quinizarin; 1, 2, 4-thATQ = purpurin; 4-h-TF = 4-hydroxy-tamoxifen.